ChemComm

ROYAL SOCIETY OF CHEMISTRY

COMMUNICATION

View Article Online
View Journal

CrossMark click for updates

Cite this: DOI: 10.1039/c5cc02371h

Received 21st March 2015,
Accepted 3rd June 2015

DOI: 10.1039/c5cc02371h

www.rsc.org/chemcomm

Amine grafted silica supported CrAuPd alloy nanoparticles: superb heterogeneous catalysts for the room temperature dehydrogenation of formic acid†

Mehmet Yurderi,[a] Ahmet Bulut,[a] Nurdan Caner,[a] Metin Celebi,[a] Murat Kaya[b] and Mehmet Zahmakiran*[a]

Herein we show that a previously unappreciated combination of CrAuPd alloy nanoparticles and amine-grafted silica support facilitates the liberation of CO-free H_2 from dehydrogenation of formic acid with record activity in the absence of any additives at room temperature. Furthermore, their excellent catalytic stability makes them isolable and reusable heterogeneous catalysts in the formic acid dehydrogenation.

Hydrogen (H_2) is considered to be a promising energy carrier for our future society as it is light-weight and has a high energy density (142 MJ kg^{-1}), almost three times higher than that of natural gas (55 MJ kg^{-1}).[1] In addition to being light weight and possessing high energy density, hydrogen is also an environmentally friendly energy vector to end users when combined with proton exchange membrane fuel cells (PEMFC), since only water and small amounts of heat are the by-products when it is utilized in PEMFC.[2] However, controlled storage and release of hydrogen are still technological barriers in the fuel cell based hydrogen economy.[1,2] In this context, formic acid (FA, HCOOH), which is one of the major stable and non-toxic liquid products formed in biomass processing, has attracted recent attention as a suitable hydrogen carrier for fuel cells designed for portable use.[3] In the presence of metal catalysts, FA can catalytically be decomposed *via* dehydrogenation ($HCOOH \rightarrow H_2 + CO_2$) and dehydration ($HCOOH \rightarrow H_2O + CO$) pathways.[3] The selective dehydrogenation of FA is indispensable for the production of ultrapure H_2, since toxic carbon monoxide (CO) produced by the dehydration pathway significantly reduces the activity of the Pt catalyst in PEMFC.[4] Recently, serious efforts have been made in the development of homogeneous catalysts for the selective dehydrogenation of FA.[5] Even though, the notable activities have been reported by some of these,[6] the difficulties met during their isolation-recovery steps hinder their practical application for on-board systems. With this concern, the current research has been focused on the development of practical heterogeneous catalysts[7,8] that exhibit significant activity under mild conditions with painless synthesis and recovery routes. In spite of the tremendous labour, the majority of the reported heterogeneous catalysts for FA dehydrogenation needs extra additives (*e.g.* HCOONa, $LiBF_4$ *etc.*,) and elevated temperatures.[7] To date, only a few heterogeneous catalysts[8] have been found to provide notable activities in the additive-free FA dehydrogenation at low temperatures. In this regard, the development of highly active, selective and reusable solid catalysts that operate at low temperatures for FA dehydrogenation in the absence of additives is of great importance. Herein, we present a facile synthesis of CrAuPd alloy nanoparticles (NPs) supported on 3-aminopropyltriethoxysilane functionalized silica, hereafter referred to as CrAuPd/N-SiO_2, and their excellent catalysis in the additive-free dehydrogenation of FA at room temperature.

CrAuPd/N-SiO_2 can reproducibly be prepared through a simple impregnation route followed by subsequent sodium borohydride ($NaBH_4$) reduction in water all at room temperature.[9] After centrifugation, copious washing with water, CrAuPd/N-SiO_2 was isolated as a gray powder and characterized by multi-pronged techniques. The molar composition of the as-prepared catalyst was found to be $Cr_{0.15}Au_{0.40}Pd_{0.60}$ (0.21% wt Cr, 1.26% wt Au and 1.65% wt Pd loadings correspond to 4.0 μmol Cr, 6.6 μmol Au and 16.0 μmol Pd, 0.98 mmol NH_2/g SiO_2) by inductively coupled plasma-optical emission spectroscopy (ICP-OES) and the ninhydrin method.[10] The conventional transmission electron microscopy (CTEM), high resolution-TEM (HRTEM), scanning TEM-energy dispersive X-ray spectroscopy (STEM-EDX) and high angle annular dark field-scanning transmission electron microscopy (HAADF-STEM) investigations were performed to examine the size, morphology and the composition of the CrAuPd/N-SiO_2 catalyst. CTEM images of CrAuPd/N-SiO_2 given in Fig. 1(a) and (b) reveal the presence of CrAuPd NPs. The mean particle size for the images given in Fig. 1(a) and (b) was found to be *ca.* 2.6 nm by the particle size analysis of >100 non-touching particles

[a] Department of Chemistry, Science Faculty, Yuzuncu Yıl University, 65080, Van, Turkey. E-mail: zmehmet@yyu.edu.tr; Web: www.nanomatcat.com
[b] Department of Chemical Engineering and Applied Chemistry, Atilim University, 06836, Ankara, Turkey

† Electronic supplementary information (ESI) available: Detailed synthesis protocols, experimental procedures, activity results, TEM, FTIR, XPS, and GC characterization. See DOI: 10.1039/c5cc02371h

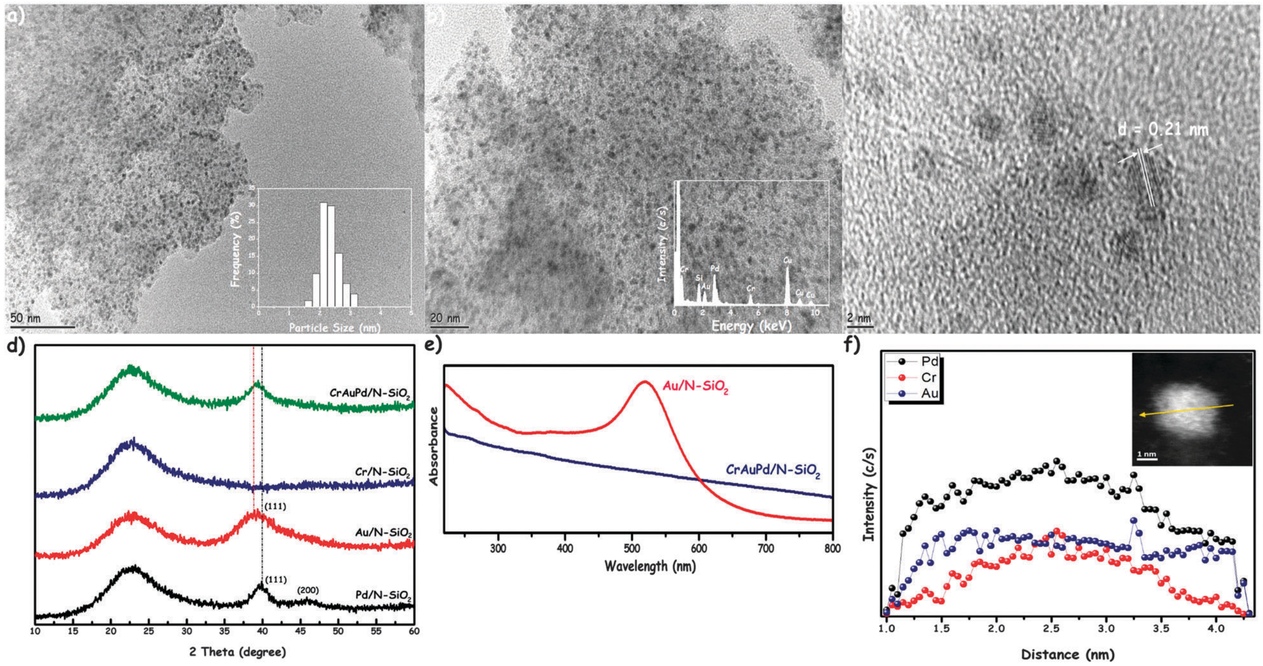

Fig. 1 (a) CTEM image and the corresponding size histogram, (b) CTEM and TEM-EDX spectrum, (c) HRTEM image of CrAuPd/N-SiO_2, (d) P-XRD patterns of CrAuPd/N-SiO_2, Cr/N-SiO_2, Au/N-SiO_2, Pd/N-SiO_2, (e) DR-UV-vis spectra of CrAuPd/N-SiO_2 and Au/N-SiO_2, (f) HAADF-STEM image and line scan analysis spectrum of CrAuPd/N-SiO_2.

(Fig. 1(a), inset). STEM-EDX analysis of a large number of different domains on the CrAuPd/N-SiO_2 surface revealed the presence of Cr, Au, and Pd in the analyzed regions (Fig. 1(b), inset). The HRTEM image of CrAuPd/N-SiO_2 given in Fig. 1(c) displays the highly crystalline nature of the NPs on N-SiO_2.

The crystalline fringe distance was measured to be 0.21 nm, which is different from the (111) spacing of the face-centered cubic (fcc) Au (0.235 nm),[8e] Pd (0.223 nm)[8e] and the (110) spacing of Cr (0.263 nm).[11] In addition to this, the powder X-ray diffraction (P-XRD) pattern of the as-synthesized catalyst (Fig. 1(d)) exhibits a diffraction peak in the position between Pd(111) and Au(111), whose position also differs from Cr(110).[11] The diffuse reflectance UV-vis (DR-UV-Vis) spectrum taken for solid powders of CrAuPd/N-SiO_2 (Fig. 1(e)) shows almost no surface plasmon resonance band for Au NPs, whereas AuN-SiO_2 has surface plasmon resonance bands near 440 nm. This surface plasmon resonance quenching caused by alloying was also observed in PdAu[8e] and PdAg[8f] alloy NPs. Furthermore, the formation of an alloy structure was also confirmed by HAADF-STEM-line analysis (Fig. 1(f)). When the distribution of Cr, Au and Pd in the randomly chosen particle was assessed by using the line scanning analysis in the STEM-EDX mode, we can clearly see the overlapping of Cr, Au and Pd signals that can be assignable to the formation of alloy structure in CrAuPd NPs. Additionally, X-ray photoelectron spectroscopy (XPS) results reveal that the binding energies for Pd 3d and Au 4f in CrAuPd/N-SiO_2 are shifted to the lower values with respect to those in Pd/N-SiO_2 and Au/N-SiO_2, respectively; whereas the Cr 2p binding energy is shifted to a higher value compared with that of Cr/N-SiO_2 (Fig. S1, ESI†). These shifts are indicative of transfer of some electrons from Cr to Pd and Au to equalize the Fermi level owing to the difference of work functions of Pd (5.67 eV), Au (5.54 eV) and Cr (4.5 eV). This electron transfer in CrAuPd/N-SiO_2 has the potential deign itself with the high activity in FA dehydrogenation (*vide infra*) as the increase in the electron density of catalytically active Pd and Au centers facilitates metal-formate formation in the FA decomposition, which enhances the rate of the catalytic dehydrogenation of FA.[12]

The catalytic activities of $Cr_{0.15}Au_{0.40}Pd_{0.60}$/N-$SiO_2$ together with its monometallic, bimetallic and trimetallic counterparts in different molar compositions were investigated in the dehydrogenation of aqueous FA solution (0.20 M in 10.0 mL H_2O) at 298 K and their results are given in Fig. 2(a)–(c). Evidently, the $Cr_{0.15}Au_{0.40}Pd_{0.60}$/N-$SiO_2$ catalyst provides a better activity than mono and bimetallic catalysts prepared by the same method. From Fig. 2(a) and (b), it is clear that Pd is the crucial active metal in all catalysts; without Pd addition $Cr_{1.0}$/N-SiO_2, $Au_{1.0}$/N-SiO_2, and $Cr_{0.49}Au_{0.51}$/N-SiO_2 catalysts show almost no activity. On the other hand, the initial activity of monometallic Pd ($Pd_{1.0}$/N-SiO_2) cannot resume as the active sites are easily deactivated by poisonous CO intermediate, which is one of the important obstacles for the application of monometallic catalysts in FA dehydrogenation.[3] Although, bimetallic $Cr_{0.48}Pd_{0.52}$/N-SiO_2 and $Au_{0.45}Pd_{0.55}$/N-SiO_2 catalysts show better activities than $Pd_{1.0}$/N-SiO_2, their performances are still far inferior to the trimetallic $Cr_{0.15}Au_{0.40}Pd_{0.60}$/N-$SiO_2$. The morphological investigation by CTEM analyses (Fig. S2, ESI†) reveals that mono and bimetallic catalysts have similar shapes and sizes with respect to $Cr_{0.15}Au_{0.40}Pd_{0.60}$/N-$SiO_2$. The enhanced catalytic activity of $Cr_{0.15}Au_{0.40}Pd_{0.60}$/N-$SiO_2$ may be attributed to its special composition and surface electronic state in the formed alloy structure,[13] which was further supported by the result of a control experiment in which the physical mixture

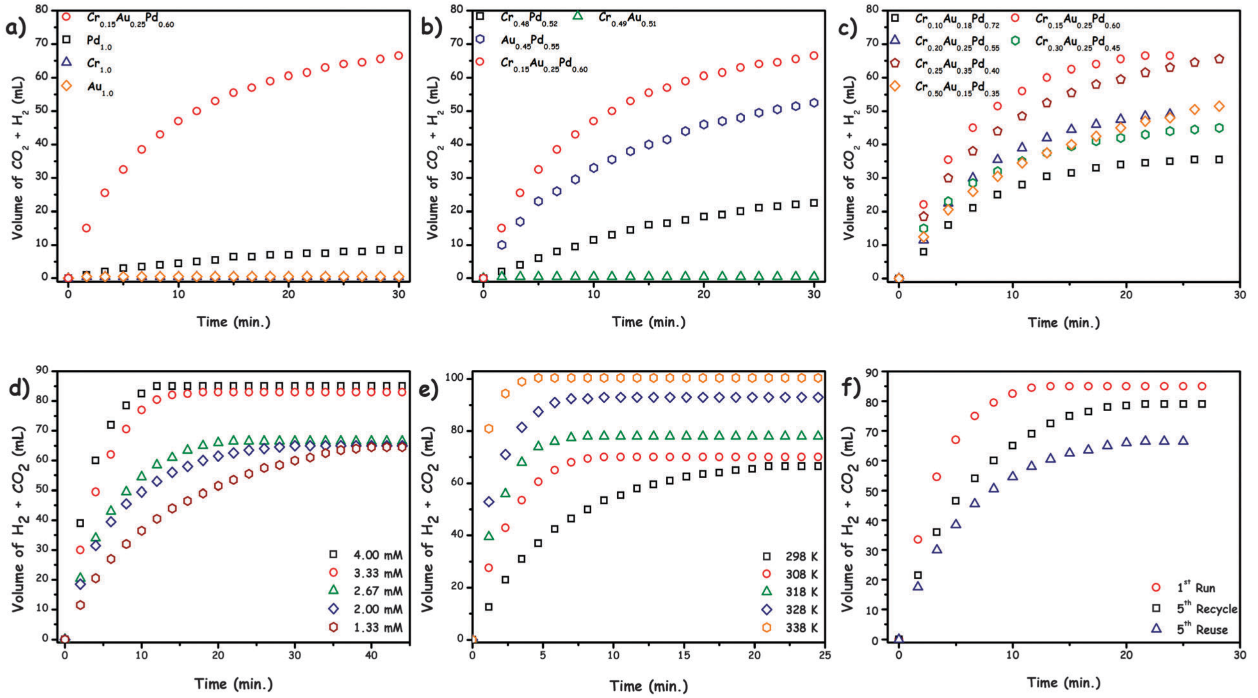

Fig. 2 The volume of gas (CO_2 + H_2) (mL) *versus* time (min) graphs for the catalytic dehydrogenation of aqueous FA solution (0.20 M in 10.0 mL H_2O) catalyzed by (a) monometallic, (b) bimetallic, (c) trimetallic catalysts (in all [catalyst] = 2.67 mM), (d) $Cr_{0.15}Au_{0.25}Pd_{0.60}$/N-$SiO_2$ catalyst at different [CrAuPd] concentrations at 298 K, (e) $Cr_{0.15}Au_{0.25}Pd_{0.60}$/N-$SiO_2$ catalyst at different temperatures, and (f) reusability and recyclability performances of the $Cr_{0.15}Au_{0.25}Pd_{0.60}$/N-$SiO_2$ catalyst in the FA dehydrogenation (0.20 M in 10.0 mL H_2O) at 298 K.

of $Cr_{0.17}$/N-SiO_2, $Au_{0.23}$/N-SiO_2 and $Pd_{0.60}$/N-SiO_2 exhibits lower activity than the $Cr_{0.15}Au_{0.40}Pd_{0.60}$/N-$SiO_2$ catalyst in FA dehydrogenation under identical conditions (Fig. S3, ESI†). The generated gas obtained during $Cr_{0.15}Au_{0.40}Pd_{0.60}$/N-$SiO_2$ catalyzed FA dehydrogenation was analyzed by gas chromatography (GC), infrared spectroscopy (FTIR) and NaOH trap experiment (Fig. S3–S6, ESI†). Their results revealed that the generated gas is a mixture of H_2 and CO_2 with a $H_2:CO_2$ molar ratio of 1.0 : 1.0 where CO was below the detection limit (*i.e.* <10 ppm). In other words, these experiments point to the important fact that CO-free H_2 generation can be achieved in the absence of additives even at room temperature from an aqueous FA solution for fuel cell applications[4] by utilizing a $Cr_{0.15}Au_{0.40}Pd_{0.60}$/N-$SiO_2$ catalyst. Fig. 2(d) shows the plot of the volume of generated gas (CO_2 + H_2) *versus* time for $Cr_{0.15}Au_{0.40}Pd_{0.60}$/N-$SiO_2$ catalyzed dehydrogenation of aqueous FA solution (0.20 M in 10.0 mL H_2O) at different catalyst concentrations ([CrAuPd]). We found that only 2.0 mol% of $Cr_{0.15}Au_{0.40}Pd_{0.60}$/N-$SiO_2$ can catalyze dehydrogenation of FA at complete conversion with an initial TOF value of 730 mol H_2 mol catalyst^{-1} h^{-1}. To the best of our knowledge, this is the highest TOF value ever reported for FA dehydrogenation at room temperature using a heterogeneous catalyst without utilizing any additives (Table S1, ESI†) and is even comparable to most homogeneous catalysts.[6] More importantly; the dehydrogenation of FA can be completed within 10 min at >99% conversion measured at 298 K. The reaction rates at each catalyst concentration were calculated from the linear portion of each plot given in Fig. 2(d). The logarithmic plot of the hydrogen generation rate *versus* catalyst concentration (Fig. S7, ESI†) gives a line with a slope of 1.13 which indicates that $Cr_{0.15}Au_{0.40}Pd_{0.60}$/N-$SiO_2$ catalyzed additive-free FA dehydrogenation is close to first-order with respect to the catalyst concentration within the investigated concentration window.

In addition to the catalyst concentration, we also investigated the effect of temperature on the rate of FA dehydrogenation by performing the catalytic reaction at different temperatures (Fig. 2(f)). It is apparent that the $Cr_{0.15}Au_{0.40}Pd_{0.60}$/N-$SiO_2$ catalyst works more effectively at elevated temperatures (>298 K), and the initial TOF values are 1280, 2030, 3360 and 4700 mol H_2 mol catalyst^{-1} h^{-1} at 308, 318, 328 and 338 K, respectively. The reaction rates for each catalyst concentration were calculated from the linear portion of each plot.

The values of observed rate constants k_{obs} determined from the linear portions of the volume of generated gas (CO_2 + H_2) *versus* reaction time plots at five different temperatures are used to obtain Arrhenius and Eyring plots (Fig. S8 and S9, ESI†) to calculate activation parameters. Using these plots, apparent activation energy (E_a), apparent activation enthalpy ($\Delta H_a^{\neq}$) and apparent activation entropy ($\Delta S_a^{\neq}$) values were calculated to be 49.8 kJ mol^{-1}, 47.4 kJ mol^{-1} and −65.1 J mol^{-1} K^{-1}, respectively. Assuming that the apparent activation parameters calculated from the macroscopic kinetic data given above are relevant to the most critical activation step in the FA dehydrogenation mechanism, one can argue that the small positive value of apparent activation energy and the large negative value of apparent activation entropy imply the presence of an associative mechanism in the transition state.[14] Then, to understand the effect of the surface grafted amine group on the catalytic reactivity of CrAuPd NPs, we conducted a control experiment, in which the activity of CrAuPd NPs supported on amine-free SiO_2 was investigated in the FA dehydrogenation under identical conditions. We found that an amine-free SiO_2 supported CrAuPd catalyst ($Cr_{0.13}Au_{0.27}Pd_{0.60}/SiO_2$) provides lower catalytic performance (TOF = 120 mol H_2 mol catalyst^{-1} h^{-1} and 42% conversion) than that of $Cr_{0.15}Au_{0.40}Pd_{0.60}$/N-$SiO_2$ (Fig. S10, ESI†). The lower reactivity of $Cr_{0.15}Au_{0.40}Pd_{0.60}$/N-$SiO_2$ can be explained by the absence of $-NH_2$ functionalities on the support material, which may have a direct impact on the FA adsorption/storage process as well as the nucleation and growth of the CrAuPd NPs on the support surface. The CTEM image of the $Cr_{0.13}Au_{0.27}Pd_{0.60}/SiO_2$ catalyst (Fig. S11, ESI†) reveals the existence of highly clumped particles with respect to $Cr_{0.15}Au_{0.40}Pd_{0.60}$/N-$SiO_2$, which shows the stabilizing effect of surface grafted amine groups.[15] Additionally, Yamashita *et al.*[16] reported that Pd or Ag@Pd NPs supported on a resin bearing $-N(CH_3)_2$ acted as more efficient organic supports than those of bearing $-SO_3H$, $-COOH$ and $-OH$ in the catalytic decomposition of FA. According to the results of their detailed mechanistic studies, it was found that O–H bond cleavage is facilitated with the assistance of the $-N(CH_3)_2$ group and leads to the formation of metal-formate species along with a $-[N(CH_3)_2H]^+$ group, which, then, undergo further dehydrogenation to produce H_2 and CO_2. In the light of these results, it is reasonable to understand that the surface grafted amine existing in our support acts as a proton scavenger and provides a basic environment around CrAuPd NPs, which benefits the O–H bond dissociation that is subsequently associated with the C–H bond cleavage from the metal-formate intermediate to release H_2.

The catalytic stability of the $Cr_{0.15}Au_{0.40}Pd_{0.60}$/N-$SiO_2$ catalyst was investigated by performing recycling and reusability experiments (Fig. 2(f)). When all of the FA was converted to CO_2 and H_2 in a particular cycle, more FA was added into the solution and the reaction was continued up to five consecutive catalytic cycles. It was found that the $Cr_{0.15}Au_{0.40}Pd_{0.60}$/N-$SiO_2$ catalyst shows high stability and retains 70% of its initial activity and provides 95% of conversion without CO generation after the 5th consecutive cycle. Isolability and reusability characteristics of $Cr_{0.15}Au_{0.40}Pd_{0.60}$/N-$SiO_2$ were also tested in the FA dehydrogenation under identical conditions. After the complete dehydrogenation of FA, the catalyst was isolated as a dark gray powder and bottled under a nitrogen atmosphere. Then, it was re-dispersed in the aqueous FA solution. This re-dispersed catalyst preserved 50% of its initial activity with 80% conversion of FA to CO_2 and H_2 even after the 5th catalytic reuse. CTEM analyses of recovered samples after 5th consecutive catalytic run of the recycling and reusability experiments (Fig. S12 and S13, ESI†) show a slight increase in the average particle size of $Cr_{0.15}Au_{0.40}Pd_{0.60}$/N-$SiO_2$ (2.9 and 4.2 nm, respectively) consistent with the observed decrease in the activity at the end of these experiments. The XPS spectrum of the reused sample shows that there is no significant change in the chemical states of Pd, Au and Cr (Fig. S14, ESI†). Moreover, ICP-OES and elemental analyses of recovered $Cr_{0.15}Au_{0.40}Pd_{0.60}$/N-$SiO_2$ catalyst samples and reaction solutions indicated that metal and $-NH_2$ contents of the catalysts remained intact after recycle and reusability experiments. Additionally, removing the $Cr_{0.15}Au_{0.40}Pd_{0.60}$/N-$SiO_2$ catalyst from the reaction solution can completely stop the dehydrogenation of FA. These results are indicative of the high stability of CrAuPd NPs against leaching throughout the catalytic runs. In summary, amine grafted silica supported CrAuPd NPs have been reproducibly synthesized and preliminary characterized by the combination of multi-pronged techniques. The resulting $Cr_{0.15}Au_{0.40}Pd_{0.60}$/N-$SiO_2$ catalyst revealed a record activity (730 mol H_2 mol catalyst^{-1} h^{-1}) and excellent conversion (>99%) converging to that of the existing state of the art homogenous catalytic systems available for the room temperature dehydrogenation of FA in the absence of any additives. Understanding of the existing synergistic effects in the $Cr_{0.15}Au_{0.40}Pd_{0.60}$/N-$SiO_2$ catalyst remains an active area of research in our group. More detailed experimental studies on the mechanism of $Cr_{0.15}Au_{0.40}Pd_{0.60}$/N-$SiO_2$ catalyzed dehydrogenation of FA are still underway. This uniquely active, selective and stable catalytic material has strong potential to be exploited in practical/technological applications, where FA is utilized as a viable hydrogen carrier in mobile fuel cell applications.

Notes and references

1 L. Schlapbach and A. Züttel, *Nature*, 2001, **414**, 353.
2 J. A. Turner, *Science*, 1999, **285**, 687.
3 M. Yadav and Q. Xu, *Energy Environ. Sci.*, 2012, **5**, 9698.
4 K. V. Kordesch and G. R. Simader, *Chem. Rev.*, 1995, **95**, 191.
5 T. C. Johnson, D. J. Morris and M. Wills, *Chem. Soc. Rev.*, 2010, **39**, 81–88.
6 A. Boddien, D. Mellmann, F. Gaertner, R. Jackstell, H. Junge, P. J. Dyson, G. Laurenczy, R. Ludwig and M. Beller, *Science*, 2011, **333**, 1733.
7 A. Bulut, M. Yurderi, Y. Karatas, M. Zahmakiran, H. Kivrak, M. Gulcan and M. Kaya, *Appl. Catal., B*, 2014, **160**, 514.
8 (*a*) K. Tedsree, T. Li, S. Jones, C. W. A. Chan, K. M. K. Yu, P. A. J. Bagot, E. A. Marquis, G. D. W. Smith and S. C. E. Tsang, *Nat. Nanotechnol.*, 2011, **6**, 302; (*b*) Z. L. Wang, J. M. Yan, H. L. Wang, Y. Ping and Q. Jiang, *J. Mater. Chem. A*, 2013, **1**, 12721; (*c*) Z. L. Wang, J. M. Yan, Y. Ping, H. L. Wang, W. T. Zheng and Q. Jiang, *Angew. Chem., Int. Ed.*, 2013, **52**, 4406; (*d*) Z. L. Wang, H. L. Wang, J. M. Yan, Y. Ping, S. II. O, S. J. Li and Q. Jiang, *Chem. Commun.*, 2014, **50**, 2732; (*e*) Ö. Metin, X. Sun and S. Sun, *Nanoscale*, 2013, **5**, 910; (*f*) S. Zhang, Ö. Metin, D. Su and S. Sun, *Angew. Chem., Int. Ed.*, 2013, **52**, 3681; (*g*) A. Bulut, M. Yurderi, Y. Karatas, M. Zahmakiran, H. Kivrak, M. Gulcan and M. Kaya, *Appl. Catal., B*, 2015, **164**, 324.
9 See the ESI† for details.
10 I. Taylor and A. G. Howard, *Anal. Chim. Acta*, 1993, **271**, 77.
11 J. He, Y. Zhang and E. Y.-X. Chen, *ChemSusChem*, 2013, **6**, 61.
12 J. S. Yoo, F. A. Pedersen, J. K. Nørskov and F. Studt, *ACS Catal.*, 2014, **4**, 1226; J. A. Herron, J. Scaranto, P. Ferrin, S. Li and M. Mavrikakis, *ACS Catal.*, 2014, **4**, 4434.
13 R. Ferrando, J. Jellinek and R. L. Johnston, *Chem. Rev.*, 2008, **108**, 845.
14 K. A. Connors, *Theory of Chemical Kinetics*, VCH Publishers, New York, 1990.
15 M. Zahmakiran, M. Tristany, K. Philippot, K. Fajerweg, S. Özkar and B. Chaudret, *Chem. Commun.*, 2010, **46**, 2938.
16 K. Mori, M. Dojo and H. Yamashita, *ACS Catal.*, 2013, **3**, 1114.

